PERGAMON

Continental Shelf Research 18 (1998) 1081–1098

CONTINENTAL SHELF RESEARCH

Beach cusp formation and spacings at Duck, USA

K. Todd Holland

Naval Research Laboratory, Code 7442, Stennis Space Center, MS 39529, USA

Received 24 October 1996; received in revised form 2 January 1998; accepted 16 January 1998

Abstract

Approximately nine years of daily video images from Duck, NC, USA, were analyzed to determine the timing of cusp formation in relation to environmental forcing and the distances separating consecutive cusp horns. 57 independent cusp events (defined as transitions from visibly smooth to cuspate topography) were observed with most of the cusps forming after storms. The temporal lag between the peak in storm intensity and cusp development was typically 3 days. Approximately half of the cusp events had formations predicted by an empirical threshold relating storm presence, breaker angle, and beach reflectivity. This threshold and other statistical observations suggest that Duck cusps form as energy conditions become more reflective, as the offshore wave angle approaches normal incidence and as the directional spread of the incident wave field becomes narrower. The standard deviation of the observed spacings relative to the mean spacing for each event was around 15% with the range in spacings for each event being typically less than half the event's mean cusp width. There were no strong statistical relationships between mean cusp spacings and environmental parameters (such as swash excursion lengths).

Keywords: Beach cusps; swash; video imaging

1. Introduction

Foreshore beach cusps, also known as swash cusps, are distinctive morphological features that exhibit short-scale (10–50 m), longshore rhythmicity (Fig. 1). Cusps have been observed at a wide variety of lakeshore and ocean beach locations around the world, and have been studied by numerous researchers (Kuenen, 1948; Guza and Inman, 1975; Werner and Fink, 1993, and many others). However, the physical mechanisms and processes governing cusp formation and spacings are still largely unresolved. The most plausible models generally involve some combination of swash mechanics (Longuet-Higgins and Parkin, 1962; Dean and Maurmeyer, 1980), edge waves (Bowen and Inman, 1969; Guza and Inman, 1975), and/or self-organization

0278–4343/98/$ – See front matter
PII S0278–4343(98)00024–7

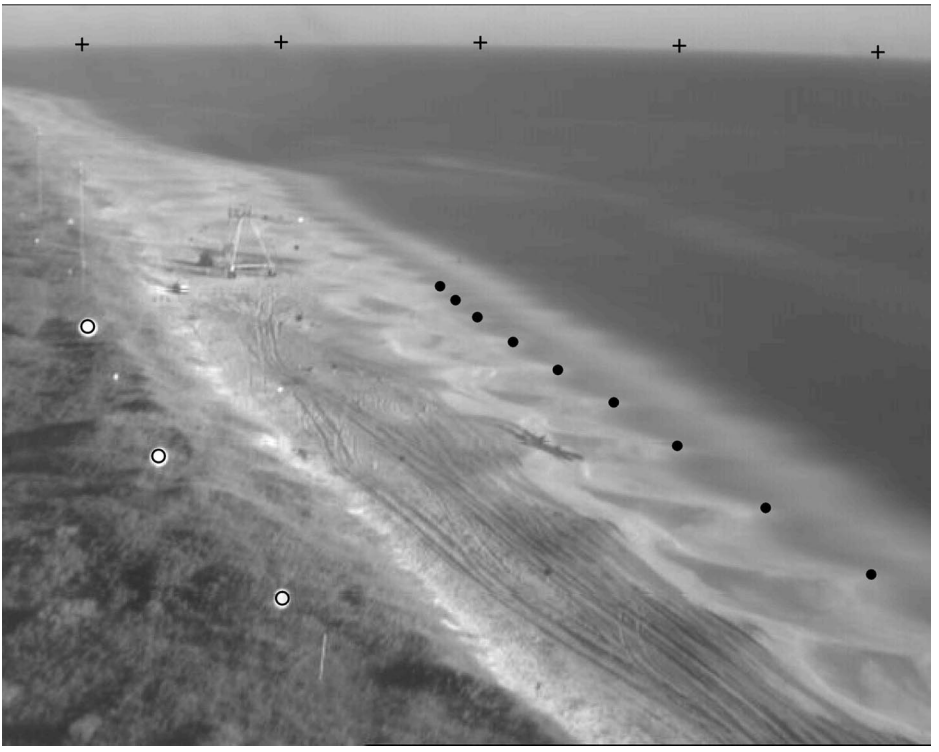

Fig. 1. Time exposure image of beach cusps at Duck, NC, USA. Image was sampled 29 September 1994. Ground control points (white circular targets) served as inputs for determination of the camera model describing the geometric relationships between image and world coordinates. Estimated control point positions (black circles) and estimated horizon positions (gray plus signs) indicate the accuracy of this model. Cusp horn positions (dark filled circles) were manually located and used to determine cusp spacings for each of the 57 cusp events.

(Johnson, 1910; Werner and Fink, 1993). In addition, a variety of descriptions of the relevant environmental variables (as opposed to mechanisms) conducive to cusp formation have been presented. Important conditions previously suggested include: reflective beach conditions (Guza and Inman, 1975; Wright et al., 1979); narrow-banded, long-crested waves (Longuet-Higgins and Parkin, 1962); normal incidence angles (Johnson, 1919; Timmermans, 1935; Longuet-Higgins and Parkin, 1962); and low tidal ranges (Shepard, 1938).

One explanation for the lack of consensus is that cusp formation is often extremely rapid. Cusps have been observed to develop from a smooth profile on time scales as short as a few minutes (Evans, 1938; Komar, 1973), although time spans on the order of one to three tidal cycles are perhaps more typical (e.g. Sato et al., 1992; Holland and Holman, 1996). Consequently, it is difficult to sample the conditions surrounding the initiation event. Since many measurements of cusp spacings and environmental

conditions have been made following cusp formation (i.e., once the characteristic rhythmicity is already apparent) and most cusp experiments have been limited to durations of only a few days, some of the prior speculation about cusp formation in association with forcing conditions may be misleading.

In an effort to measure cusp formation conditions, beach cusp development and spacings were closely monitored (to the nearest day and to the nearest meter) at Duck, NC, USA, over an 8.9 yr period. The objectives of this study were: (1) to document the environmental conditions conducive to cusp formation; and (2) to quantify the degree of uniformity of cusp spacings at this site. An empirical relationship defining the timing of cusp formation is given and statistics describing the variation in observed cusp spacings are presented. Although the measurements necessary to distinguish conclusively between the various hypotheses of cusp development were beyond the scope of this data collection effort, many of the findings in this study are pertinent to certain aspects of the different theories of cusp formation.

2. Study site and methods

The concept of using remote sensing methods to monitor cusp formation is not new. Darbyshire (1977) mentions his intention to record the 'actual formation' of cusps using time-lapse photography. Nishi and Sato (1991) monitored cusp features over a six-year period using photographs taken from the top of Mt. Kaimon-dake. More recently, Sloop (1995) used video monitoring techniques to document one month of cusp behavior at Longboat Key, FL. What distinguishes this study from these and other prior works is the extent of the temporal coverage (nearly nine years), the relatively rapid sampling interval (daily), and the quantitative measurement of both the cusp spacings and corresponding environmental conditions at the time of cusp formation.

Video images and field data were collected between 7 October, 1986 and 11 September, 1995 at the US Army Corps of Engineers Field Research Facility (FRF) on the Outer Banks of mid-Atlantic coast of the United States (Birkemeier et al., 1985, Fig. 2). This site is typically a barred beach with a relatively steep (1:12.5) foreshore. The median grain size of foreshore sediments is 1.0 to 1.5 ϕ. Offshore, the bottom slope near the 8 m depth contour approaches 1:164. Low (<1 m) southerly swell dominates in summer months with higher waves and periods of intense storms (typically from the northeast) occurring during the rest of the year. Tides are semi-diurnal and have an average range of about 1 m.

2.1. Argus image database

The primary data source used in this investigation were time-exposure images from the Duck Argus image database that has been developed by the Coastal Imaging Lab at Oregon State University (Holman et al., 1993). Time exposures (Fig. 1) are digital images that represent the average (over a twelve-minute period) image intensity within a camera's field of view. In surf-zone regions, these intensity patterns are

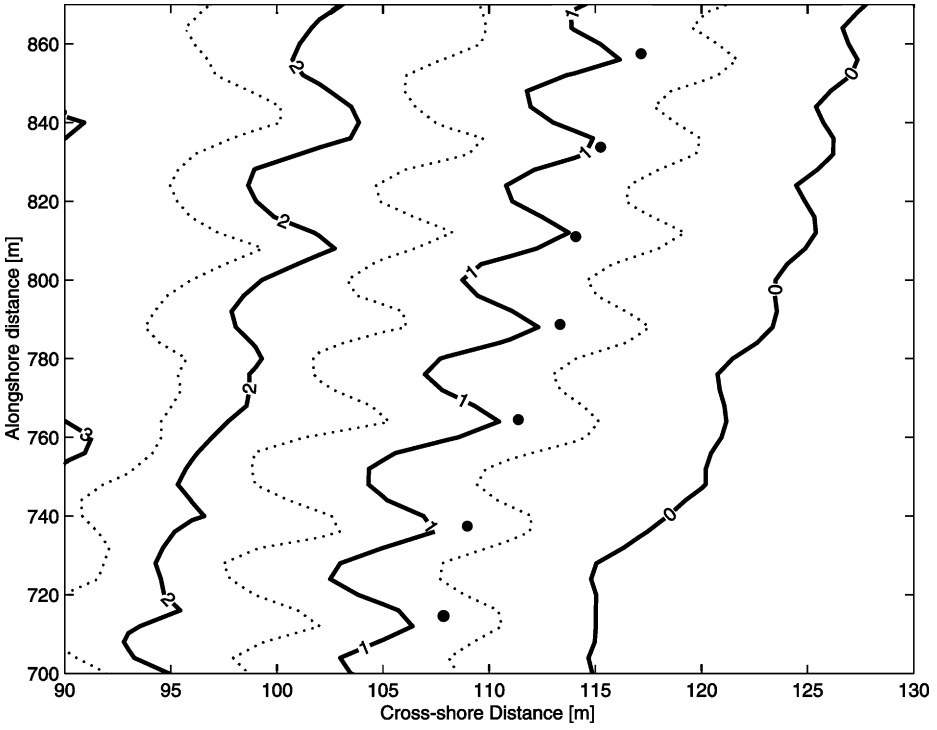

Fig. 2. Comparison of foreshore topographic contours with cusp horn positions (circles) estimated using the video technique. Elevations (in meters) relative to mean lower low water are indicated. For this example, the average cusp spacing determined from the survey data was 24.2 m and the average spacing determined using the video method was 23.8 m.

representative of the amount of wave energy dissipation; and therefore, brighter pixels reflect, in an average sense, regions of preferential wave breaking (Lippmann and Holman, 1989). Since a major control on wave breaking is water depth, the intensity variations within a time exposure image serve as a proxy for variations in bathymetry. Although time exposures are typically used to identify sand bar structures, this image type is also useful in the determination of beach cusp morphology. Cusp horns and embayments are readily identifiable in the time exposure imagery and cusp widths are often emphasized by intensity patterns reflective of swash circulation over well-developed cusp morphology (see, for example, Fig. 2 from Inman and Guza (1982) or Fig. 2 from Holland and Holman (1996)).

The Duck Argus camera is mounted on a 43 m tower. Over 2700 images from this camera were examined to isolate cusp formation events. These images were sampled at least daily (imagery subsequent to March 1993 were sampled hourly during daylight hours), apart from a few instances when the camera was malfunctioning. The longest downtime interval was 175 days during the winter of 1992. Individual formation events were defined as obvious signs of cusp presence following imagery that

showed no visible indications of cusps or showed otherwise monotonic topography. This definition required that changes within an existing cusp field following initial formation were not viewed as independent (in some cases, the remnants of a cusp field within the active foreshore region were visually apparent for up to two months). Therefore the number of images that showed cusps greatly exceeded the number of identified cusp events. Additionally, the resolution of the video imagery (described below) was not sufficient to detect small-scale perturbations in developing cusp systems. Therefore, it is possible that cusp events with very small spacings (<5 m) or very small amplitudes (<0.1 m vertically) may have gone undetected.

Using the definition of a formation event given above, the exact timing of cusp development for each event was selected (following the suggestion of Longuet-Higgins and Parkin, 1962) to be the occurrence of the high tide prior to the first visible indication of cusp presence. Since the tides at Duck are semi-diurnal and the imagery was sampled during daylight hours only, this formation time was often at night. It is important to note that this timing choice had no effect on which images were used to identify cusp presence nor did it have an appreciable effect on the accuracy of the cusp spacing nor is it a statement that cusps only form at high tide; it was solely a numerical constraint to allow the definition of the vertical coordinate of the measured cusp field. Cusp destruction events were defined in the same manner, however, given the difficulty in accurately estimating the exact timing of cusp disappearance (using any means, visual or otherwise), all measurements of cusp persistence should be regarded as approximate.

The video technique used to determine cusp spacings is the video image rectification procedure described by Holland et al. (1997). Briefly, corresponding image and spatial measurements of ground control point markers (Fig. 1) were used to define a camera model describing the geometrical relationships between image and spatial coordinates within the camera field of view. Given that the data used to determine cusp spacings were derived from video images, a transformation from two-dimensional pixel locations to three-dimensional cusp horn positions was required (Holland et al., 1997, Eq. (3)). This transformation is not possible when using only one camera (i.e. the corresponding system of equations relating image and spatial coordinates is underdetermined) unless one of the spatial coordinates (x, y, or z) is constrained. Therefore a constraint that the elevation (z) of the most landward peak in the cusp horns (an easily identifiable position) be coincident with the water level elevation at the time of cusp formation (defined above to be the prior high tide) was applied. This elevation constraint allowed the absolute spatial positions of cusp horns to be determined from manually located pixel coordinates.

The application of this technique was restricted to the foreshore region within the view of the camera that had an alongshore pixel footprint (the spatial scale of a pixel mapped to the ground plane) of less than 2.5 m. Since resolution decreases with distance from the camera, this restriction minimized errors in cusp width estimates resulting from inadequate image resolution. The average footprint over the alongshore region of coverage (~ 250 m in length) was 1.1 m, however, since cusps were located with sub-pixel accuracy, the accuracy in the cusp width estimate is much better, on the order of 0.5 m. Repeated determination of cusp widths for a single image

indicated that the repeatability in the digitization of the cusp spacing is within 5%. A contour map demonstrating one example of the close correspondence between surveyed and video estimated cusp positions is shown in Fig. 2.

The accuracy of this method is only weakly sensitive to the error in the high tide elevation constraint. For a camera oriented looking directly alongshore and centered on a cusp, the error in the absolute alongshore position of one of the cusp horns, Δy, introduced by using an incorrect elevation estimate, Δz, scales as $\Delta y \cong \Delta z/\tan(\tau)$, where τ is the camera tilt relative to the horizontal. Note that as vertical camera orientations are approached the horizontal positioning error goes to zero. Using the tilt of the Duck Argus camera system (about 10°), a 1.5 m elevation error (a maximum spring tidal range) would result in almost 10 m of error in the absolute position estimate. However, the relative spacing error, $\Delta\lambda$, representing the difference between estimated and actual cusp width estimates and resulting from using the incorrect elevation, is much smaller. It scales as $\Delta\lambda/\lambda \cong \Delta z/d$, where λ is the actual cusp width and d is the distance between the camera and the cusp. For the Duck sampling system, where the average distance from the camera to cusp was approximately 250 m, the same 1.5 m error would yield a $\Delta\lambda$ on the order of 0.15 m for a 25 m cusp spacing. Therefore inaccuracy in the elevation constraint due to timing mismatch or exclusion of wave setup has only a small effect of the accuracy of the video-derived cusp wavelengths.

2.2. Supplemental measurements

Data representative of environmental conditions preceding and during cusp formation were also utilized. Nearshore hydrodynamic conditions were determined for each of the cusp events from the FRF wave, current, and water level data archives. These statistics included offshore significant wave height, H_s, calculated as four times the sea surface standard deviation from pressure measurements sampled in 8 m depth; offshore wave period at the maximum energy peak, T_p; offshore wave direction, α, as obtained from a nine-element linear array of bottom mounted pressure gauges in 8 m depth; breaker height, H_b, calculated from a pressure gauge or Baylor staff approximately 140 m offshore in 2 m depth; breaker period, T_b, at the same location; and mean water level, h, from the primary tide station at the seaward end of the FRF pier. Half-power bandwidths of the main peak for both direction and frequency ($\Delta\alpha$ and Δf, respectively) were also calculated from frequency-directional spectra estimated using data from the 8 m array. Foreshore beach slopes, β, were determined from bi-monthly bathymetric profiles sampled using the FRF's Coastal Research Amphibious Buggy (CRAB).

Given that observations of swash excursions were not available, empirical estimates of swash excursion were derived following the relationship given in Holman and Sallenger (1985, Fig. 7, Table 1).

$$R_s^v/H_0 \approx 0.9\frac{\beta}{\sqrt{H_0/L_0}} \tag{1}$$

where R_s^v is the significant swash height; and H_0 and L_0 are the offshore significant wave height and wavelength, respectively, measured in 20 m depth. This relationship was determined specifically for the Duck site and was shown statistically invariant over all tide levels. Additionally, Holman (1986) showed a lack of significant change in regression coefficients for similar swash statistics by using incident wave height and period sampled in 6 m depth. Resio (1987) using the same dataset, indicates that using wave characteristics sampled in very shallow water actually degrades the performance of these type predictors. Therefore, for this study, swash excursion, S_x, was estimated from Eq. (1) as

$$S_x = R_s^v/\beta \approx 0.9\sqrt{H_0 L_0} \tag{2}$$

using $H_0 = H_s$ and $L_0 = gT_p^2/2\pi$.

3. Results

3.1. Timing and controls on cusp formation

Fifty seven independent examples of cusp formation were identified over the 8.9 yr period. In general, the cusps developed rapidly, going from indistinguishable to well developed over 3 consecutive (daily) samples. There was little indication that the cusps became more equally spaced over time, although a few examples of cusp additions to the ends of existing cusp systems were observed (e.g., 16–18 June 1993). Close inspection of cusp events occurring during the interval for which hourly imagery was available revealed no indication of well-developed cusps forming on timescales of less than a few hours. Cusp degradation was typically on the order of five to ten days, although in many instances cusps persisted for over a month. The average time interval between cusp development events was 55 days, with a minimum time of 6 days and a maximum time of 269 days.

Cusps were observed to develop typically during the more energetic fall, winter, and spring months and showed a close association with storms (Fig. 3). There was no indication that cusp size (detailed below) was seasonally distributed. Most cusps generally formed one to three days after the peak in storm intensity with no obvious differences in the value of this lag between larger (spacings > 25 m) and smaller (spacings $\leqslant 25$ m) cusps (Fig. 4). However, nine of the events (16%) occurred well after (defined to be more than 10 days) the most recent storm (defined to be an interval of more than 6 h for which $H_s > 1.5$ m).

The offshore (8 m) environmental conditions measured at the time of initial cusp formation, during the preceding storm, and typical of the Duck site are illustrated in Fig. 5. Offshore significant wave heights during formation (Fig. 5a) were typically $\leqslant 1$ m and were obviously less than the peak storm wave heights (Fig. 5b), implying that the cusps formed as wave heights diminished (the temporal rather than statistical version of this correlation is shown below). However, the distribution of H_s values during cusp formation did not differ significantly (at 95% confidence using

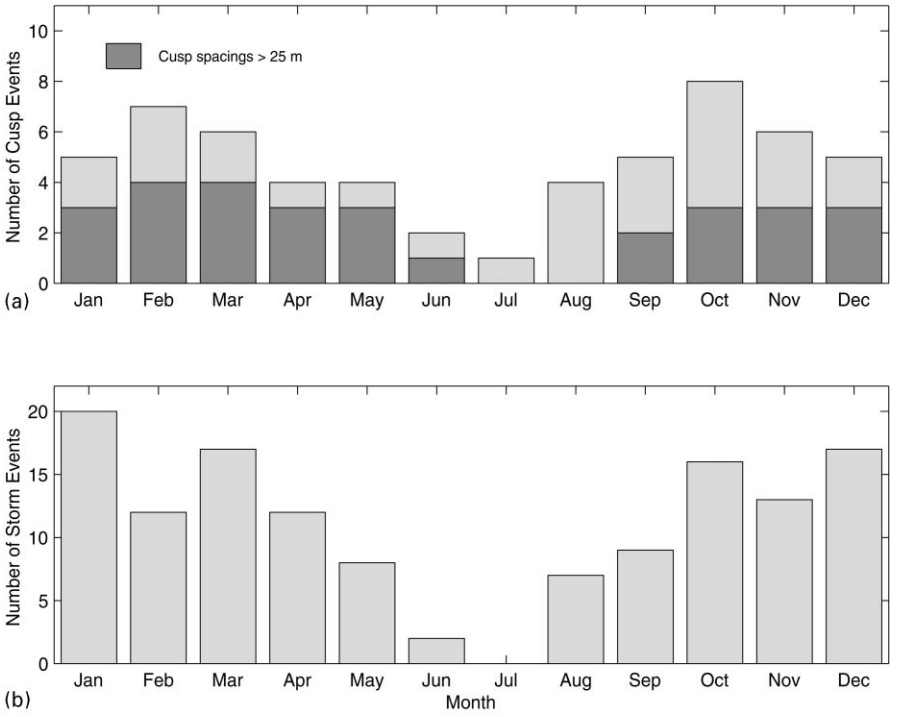

Fig. 3. Distribution of (a) cusp events and (b) storm events with respect to month of year. Storms were defined as offshore significant wave heights greater than 1.5 m.

the Kolmorogov–Smirnov goodness-of-fit test) from distribution of all H_s measurements over the period of the study, suggesting that the wave heights during formation were not unusual. Offshore incident wave angle (Fig. 5c) and offshore wave period (Fig. 5d), however, did show significantly different distributions from the corresponding overall distributions, especially at the modes of the cusp event distributions. The α values measured in 8 m depth were dominantly shore normal with 83% of the α values between -12° and 12° from normal incidence.

Offshore incident frequency spread and directional spread were also examined as controlling factors in cusp formation at Duck. The directional spread during cusp formation (Fig. 5e) as given by the half-power bandwidth statistic, $\Delta\alpha$, showed no obvious signs of being dominantly narrow-banded when compared to the overall distribution and did not differ significantly from the distribution of all $\Delta\alpha$ measurements. The frequency spread distribution, however, given by the half-power bandwidth statistic, Δf (Fig. 5f) was generally larger than the long-term distribution at small values and was significantly different using the goodness-of-fit test (the probability that the distributions were identical is only 0.5%). The half-power bandwidth distributions at the storm peaks (not shown) were not statistically different from those during cusp formation indicating that storm conditions were not particularly narrow banded.

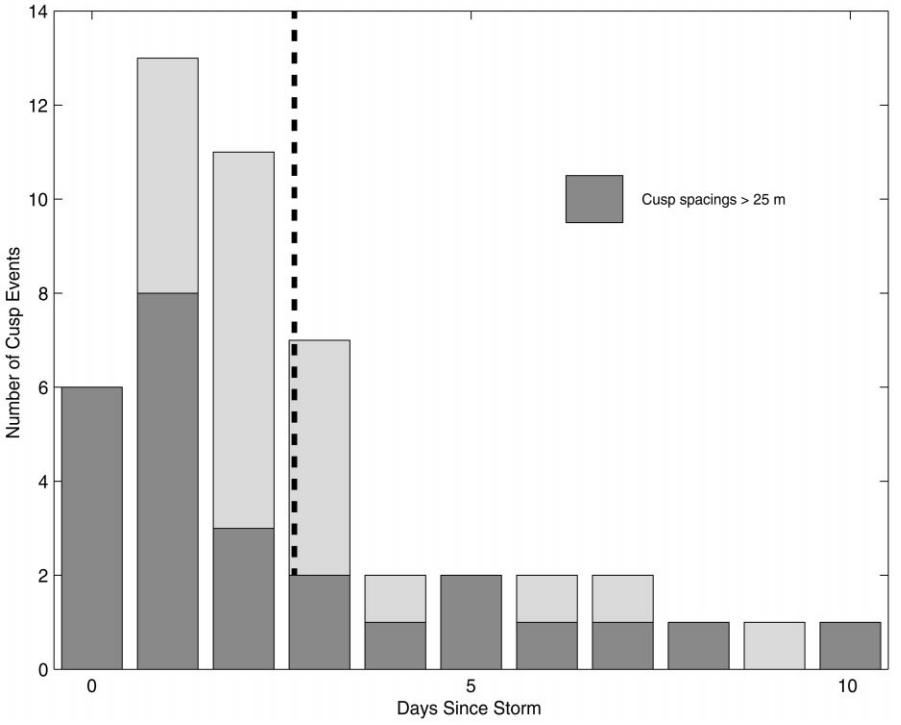

Fig. 4. Distribution of the onset of cusp events as a function of days since the peak in storm intensity. The mean value is indicated by the dashed line. Cusps with spacings >25 m are also shown.

Surf-zone and shoreline environmental conditions are shown in Fig. 6. Breaker heights and periods (Fig. 6a and b) mimicked offshore heights and periods (Fig. 5a and d). In a non-dimensional sense, these waves were small relative to the overall beach system in terms of the surf-scaling parameter, $\varepsilon = a_b\omega^2/g\tan^2\beta$ (where $a_b = H_b/2$ is the incident wave amplitude near the breakpoint, $\omega = 2\pi/T_b$, g is the acceleration of gravity and β is the beach slope). Approximately 68% of the wave conditions were categorized as reflective following the definition suggested by Wright et al. (1979) that $\varepsilon < 2.5$. The maximum value of ε was 15.1. Incident angles at the breakpoint (Fig. 6c), obtained by refracting offshore angles using Snell's law, were almost exclusively shore normal with only one event being outside the window of $\pm 12^\circ$ from shore normal and were significantly narrower than the corresponding distribution representative of conditions over the 8.9 yr period. The swash excursion distribution for conditions during cusp formation (Fig. 6d) mimicked the form of the wave height distributions and did not significantly differ from that of the entire study period.

The qualitative association between storms, incidence angle, and cusp formation can be more explicitly depicted by examining the timing of the cusp events in relation to the time series of H_s, α_b, and ε. The example subset of data shown in Fig. 7 relates

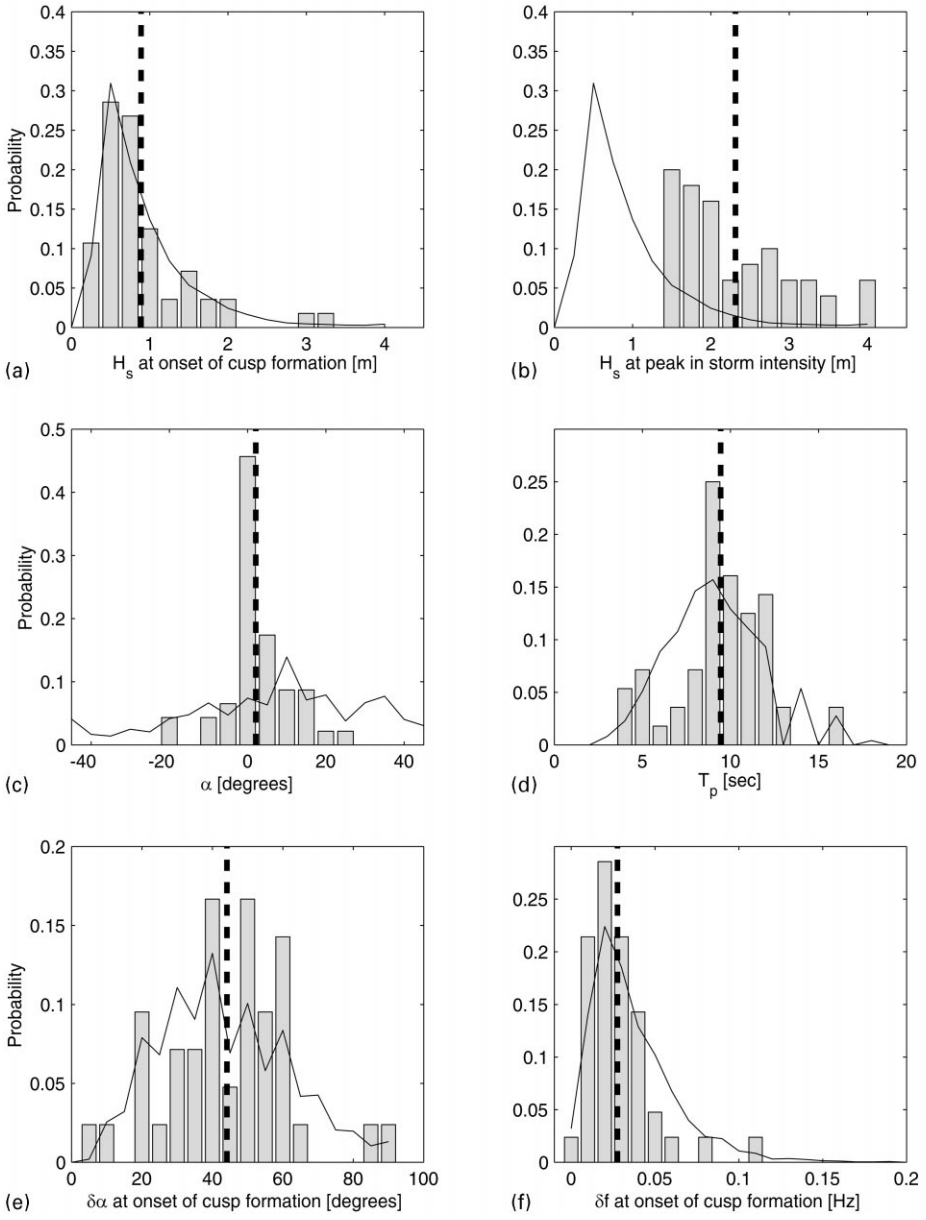

Fig. 5. Distribution of offshore environmental parameters at the time of cusp formation: (a) significant wave height, (b) peak wave height, (c) incidence angle, (d) peak wave period, (e) half-power directional bandwidth, (f) half-power frequency bandwidth. Mean values are indicated by the dashed lines. Probability distributions of hourly samples over the 8.9 study interval are given by the solid lines.

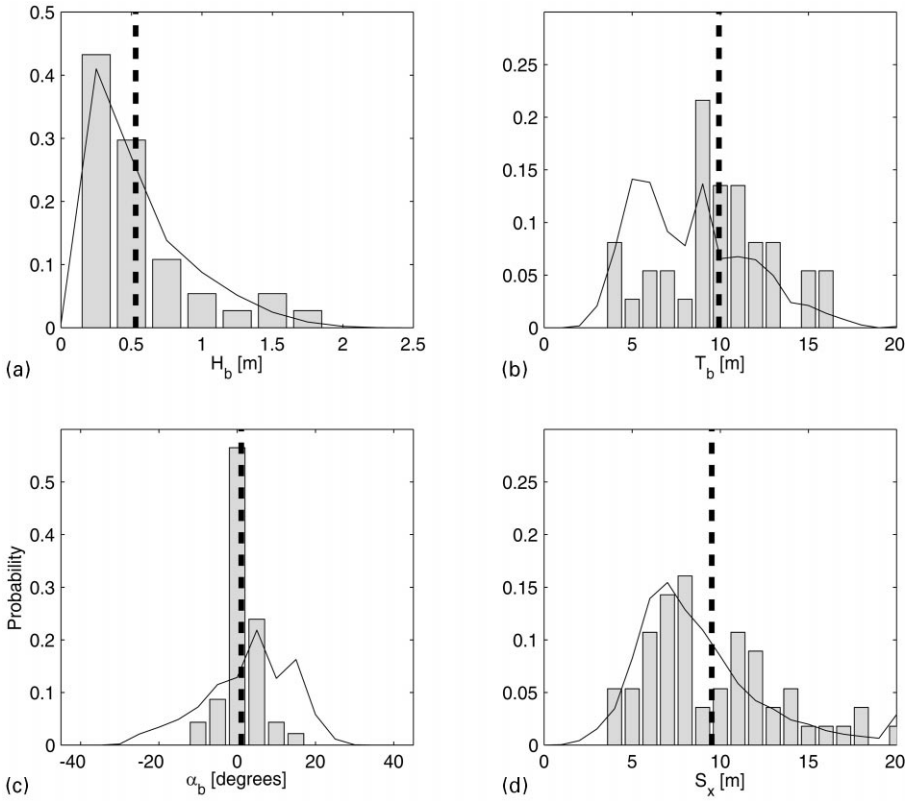

Fig. 6. Distribution of breakpoint and shoreline environmental parameters during cusp formation events: (a) breaker height, (b) breaker period, (c) breaker angle, (d) swash excursion length. Mean values are indicated by the dashed lines. Probability distributions of hourly samples over the 8.9 study interval are given by the solid lines.

wave conditions between 01 November 1991 and 30 March 1992 to the formation times of eight cusp fields (of which only five were independent events having developed from topography with no visible cusp remnants). The time intervals over which cusps were visually apparent are also shown. Close inspection of the time series shows that for the majority of events, cusps formed during the transition from storm (previously defined) to low wave energy conditions as breaker angle passed through normal incidence. The preference of nearly normal wave conditions is particularly clear for several events (e.g. 11 November 1991, 11 December 1991, and 01 January 1992) as indicated by the close timing between cusp formation and minimum absolute breaker angles. In general, wave conditions were not dissipative as most of the events had ε values <5. However, these three criteria (storm subsidence, normal incidence, and mildly reflective conditions) cannot be considered completely restrictive as there were times that cusps developed under different conditions (e.g. note the large angles

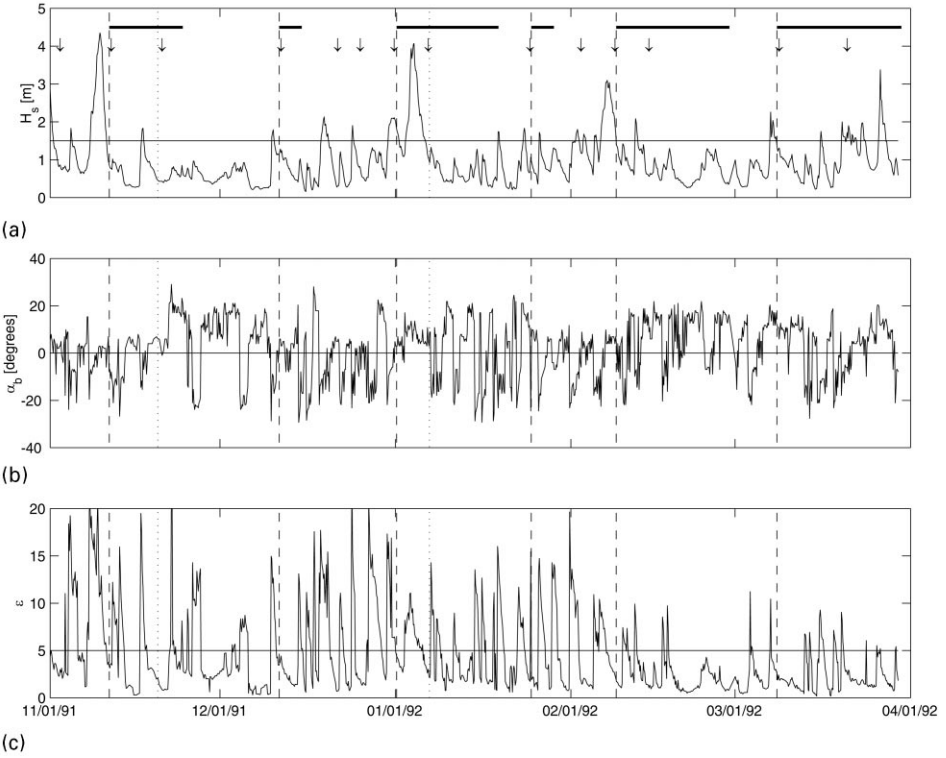

Fig. 7. Time series of (a) offshore significant wave height, H_s, (b) breaker angle, α_b (0° = normal incidence), and (c) surf-scaling parameter, ε, for the 1991–1992 storm season. Observed cusp events are indicated by the dashed and dotted vertical lines. Downward pointing arrows indicate the start of cusp formation events predicted by Eq. (3). Cusps apparent on 18 November and 07 January were not viewed as independent of the preceding event (see text). Cusp durations are indicated by the thick horizontal bars. In the top and bottom panels, the storm threshold (1.5 m) and a threshold for reflective conditions ($\varepsilon < 5$) are shown.

for 08 March 1992) and there were a several instances where no cusps developed when preferred conditions occurred (20 December 1991 and 30 March 1992, for example).

Using the entire data set, an empirical relation was developed to establish the typical threshold criteria for cusp formation at Duck as a function of storm presence, reflective conditions, and normal incidence. This relationship was defined for conditions favorable to cusp formation as:

$$\cos(3|\alpha_b|)/\varepsilon \geqslant 0.16 \tag{3}$$

following within three days of a storm event. A binary time series of cusp formation was created where each of the 57 cusp events were set to one and zero for all other times. A corresponding time series describing wave conditions was created to describe observations in terms of Eq. (3). This time series was zeroed for time intervals outside the three-day window following the peak in storm intensity (previously defined) to

include storminess as an input condition. Over the study period, of 172 possible storms identified, 74 had conditions favorable to cusp formation. Of those 74 predicted events, 35 could be directly identified with observed cusp formation suggesting that the threshold criteria are applicable to nearly half of the Duck cusp events. An example of the predictions compared to observations is given in Fig. 7a. Given that some predicted formation events occurred over time periods where the prior cusp field was still remnant (see dotted lines in Fig. 7a), the accuracy of the empirical predictor is possibly higher. The cross-association time scale (temporal lag) of cusp formation relative to the time series given by the left-hand side of Eq. (3) was 0.1 days (cusps lagging storms) indicating that the temporal accuracy of the predictor is high.

3.2. Cusp spacings

For each event, several statistics describing the measured cusp field were calculated including the number of cusp spacings, the average cusp spacing, $\bar{\lambda}$, the maximum cusp spacing, λ_{max}, the minimum cusp spacing, λ_{min}, and the standard deviation of the cusp spacings, σ. On average, a set of 6.2 cusps developed within the approximately 250 m region monitored by the camera; at most, 11 cusps within a single set were observed. The overall distribution of mean cusp spacings for observed cusp events (Fig. 8) was nearly uniform between 17 and 35 m. The measured mean spacings had a minimum of 12.4 m, a maximum of 38.8 m, and a mean of 25.8 m. The average value of the measured standard deviations of the cusp fields was 3.8 m. The distribution of all measured cusp spacings was similar with a mean of 24.9 m, but smoother with broader tails (not shown).

The uniformity of the cusp systems was described by two statistics. The coefficient of significant deviation, c_σ, describes the average variation within a cusp system as the measured standard deviation of spacings within the cusp field normalized by the average cusp spacing. Rasch et al. (1993) defines a similar statistic, the coefficient of variational width, c_{vw}, as

$$c_{vw} = \frac{(\lambda_{max} - \lambda_{min})}{\bar{\lambda}} . \tag{4}$$

A coefficient of variational width value of 0.5 (0.25) suggests that the maximum variation of the distances between individual cusps is half (one-quarter) the average spacing of the cusp system. Average (maximum) values over the experiment for c_σ and c_{vw} were 0.15 (0.35) and 0.40 (0.98) respectively. These mean values closely correspond to the mean values given by Rasch et al. (1993) for both the Danish coast and for some prior publications.

Comparison of mean cusp spacings with the parameters describing the environmental conditions at the time of cusp formation showed no strong statistical correlations. No significant linear relationships (defined as r^2 correlation values being significantly different from zero with 95% confidence) between $\bar{\lambda}$ and T_p, α, β or ε were observed. Significant correlation was observed for the linear relationships between $\bar{\lambda}$ and both H_s and H_b, however, the regression explained less than 12% of the total variation of the data about the mean. Relationships determined for mean cusp spacing

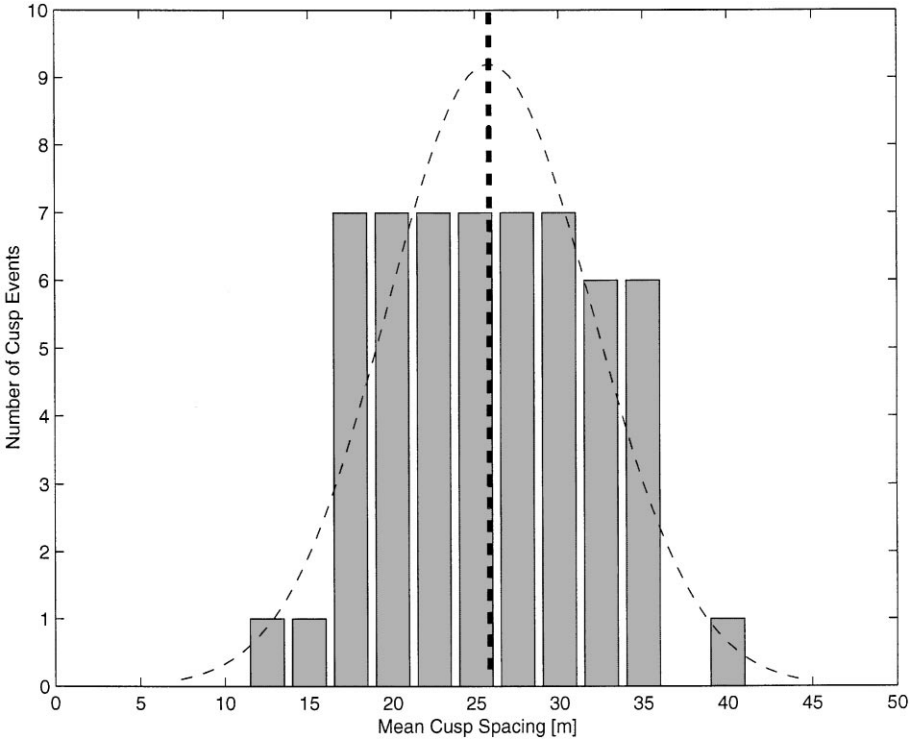

Fig. 8. Distribution of mean cusp spacings, $\bar{\lambda}$, measured for each event over the nine year study. The dashed lines indicates the mean value and a best fit Gaussian curve.

as a function of three nonlinear parameters: $0.9\,(H_0L_0)^{1/2}\,\beta$ (the approximation for R_s^v in Eq. (1)), $0.9\,(H_0L_0)^{1/2}$ (the approximation for S_x in Eq. (2)) and $2L_0\beta$ (an appropriate length scale for subharmonic edge waves on a plane beach), are shown in Fig. 9 and indicate significant correlations for all three parameterizations. Although these trends do reveal some degree of association between cusp spacing and plausible environmental forcing parameterizations, the comparisons are quite scattered (no more than 35% of the observed variation was explained) and the intercepts are not zero suggesting that other factors are likely important.

4. Disscusion

The findings of this study support several previously suggested, qualitative statements of conditions preferential to cusp development. The first is that wave incidence normal to the beach is required. This characteristic, which was first stated by Palmer (1834), and supported by the month-long observations of Longuet-Higgins and Parkin (1962) from the south coast of England, is clearly demonstrated in the Duck

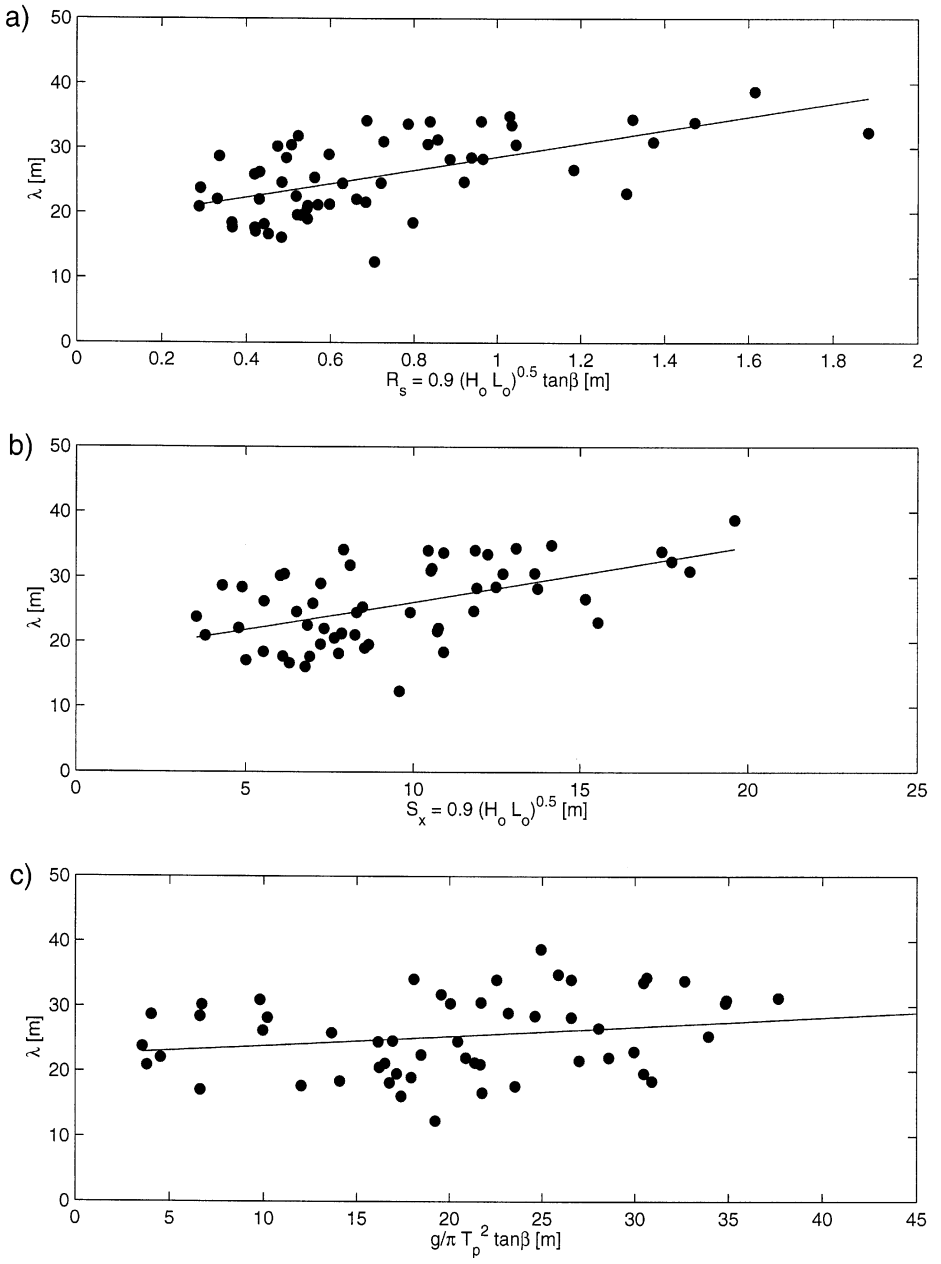

Fig. 9. Mean cusp spacing, $\bar{\lambda}$, as a function of (a) runup height, (b) swash excursion length, and (c) plane-beach approximation for wavelength of a mode 0 subharmonic edge wave. The corresponding r^2 correlation values are 0.36, 0.29, and 0.10. The linear trends explain 35%, 29% and 9% of the total variance respectively.

observations with 98% of the cusp events having breaker angles of less than 12° as compared to an expectation of 66% for typical conditions. Numerous other researchers agree with this requirement including Jefferson (1899), Johnson (1910), Timmermans (1935), and Shepard (1963). The second characteristic is that reflective conditions (as expressed by the surf-scaling parameter, ε) are necessary for cusp formation (Guza and Inman, 1975; Wright et al., 1979). This research found no cusps formed during dissipative conditions (defined as $\varepsilon > 20$), although dissipative states are common for this beach. Lastly, a significant dependence on frequency narrow-bandedness (often referenced as 'clean' conditions) was indicated. An incident wave field with a relatively narrow frequency spread has been cited as a possible requirement for cusp formation through the excitation of subharmonic edge waves (Guza and Inman, 1975).

The results also emphasized the importance of storms in cusp formation which appears to be a previously undocumented although not unexpected observation. The data showed a clear pattern of cusp formation 2–4 days following a peak in storm intensity. Qualitatively, cusps at Duck begin to form as wave heights diminish, frequency bandwidth decreases, and breakers become normally incident. Storms may serve as controlling factors that flatten the topographic template over which cusps develop and perhaps simplify the hydrodynamic forcing. Normal incidence is likely an important factor because the potential for the generation of strong alongshore currents is minimized, thereby allowing cusps to develop under dominantly cross-shore flow. Taken as a whole, these observations (and the empirical model) quantitatively define the generalized conditions preferable to cusp formation.

Unfortunately, even these long-term, comprehensive observations of forcing and response do not allow quantitative testing of the validity of any present cusp formation model. The investigation of edge wave development and their influence on cusp development takes more detailed measurements than were available for this study (see Holland and Holman, 1996). And a stronger link between cusp spacings and swash excursions (determined directly rather than empirically as in this study) must be established for conclusive evidence of cusp formation by self-organization. Even though the cusp spacing measurements and the establishment of a quantitative threshold for cusp formation may be used as diagnostic characteristics that restrict the causative mechanism of cusp formation, a different approach is needed. An investigation of three-dimensional sediment transport during cusp formation as a function of hydrodynamic forcing is planned and I hope to present evidence from this type of study in a future work.

5. Summary

Long-term observations of cusp development and persistence at Duck, NC, USA, indicate that cusps typically form following storms (with an average lag of 3 days) as beach reflectivity increases and breaker angle decreases. A significant dependence on narrow-bandedness (in frequency) was also observed. Comparison with environmental conditions around the time of cusp formation indicates that approximately

half of the observed cusp events could be predicted using an empirical threshold criterion relating offshore wave height, breaker angle, and a surf-scaling parameter. In contrast to prior studies, no strong correlations were observed between mean cusp spacings and various environmental parameters hypothesized to control cusp wavelengths.

Acknowledgements

The Argus imagery critical to the success of this project was graciously provided by Dr. R. A. Holman of the Coastal Imaging Lab at Oregon State University whose research is supported by the Office of Naval Research, the US Geological Survey, and the Mellon Foundation. The FRF data were provided by the Field Research Facility of the US Army Corps of Engineers Waterways Experiment Station's Coastal Engineering Research Center. Additional thanks go to Joan Mead for tracking down numerous articles on beach cusps. The base funding to the Naval Research Laboratory for the preparation of this manuscript was provided by the Office of Naval Research.

References

Birkemeier, W.A., Miller, H.C., Wilhelm, S.D., DeWall, A.E., Gorbics, C.S. 1985. A user's guide to the Coastal Engineering Research Center's (CERC's) Field Research Facility. 85-1, Coastal Engineering Research Center, U.S. Army Corps of Engineers Waterways Experiment Station, 136 pp.

Bowen, A.J., Inman, D.L., 1969. Rip currents, 2. Laboratory and field observations. Journal of Geophysical Research, 74 (23), 5479–5490.

Darbyshire, J., 1977. An investigation of beach cusps in Hell's Mouth Bay. In: M. Angel, (Ed.), Voyage of Discovery: George Deacon 70th Anniversary Volume. Pergamon Press, New York, pp. 405–427.

Dean, R.G., Maurmeyer, E.M., 1980. Beach cusps at Point Reyes and Drakes Bay Beaches, California. In: B. L. Edge, (Ed.), Proceedings of the 17th Coastal Engineering Conference, ASCE, Sydney, Australia, pp. 863–884.

Evans, O.F., 1938. The classification and origin of beach cusps. Journal of Geology, 46, 615–627.

Guza, R.T., Inman, D.L., 1975. Edge waves and beach cusps. Journal of Geophysical Research 80 (21), 2997–3012.

Holman, R.A., 1986. Extreme value statistics for wave run-up on a natural beach. Coastal Engineering, 9, 527–544.

Holland, K.T., Holman, R.A., 1996. Field observations of beach cusps and swash motions. Marine Geology, 134 (1–2), 77–93.

Holland, K.T., Holman, R.A., Lippmann, T.C., Stanley, J., Plant, N., 1997. Practical use of video imagery in nearshore oceanographic field studies. IEEE Journal of Oceanic Engineering 22 (1), 81–92.

Holman, R.A., Sallenger, A.H., Jr. 1985. Setup and swash on a natural beach. Journal of Geophysical Research 90 (C1), 945–953.

Holman, R.A., Sallenger, A.H., Jr., Lippmann, T.C., Haines, J.W., 1993. The application of video image processing to the study of nearshore processes. Oceanography 6 (3), 78–85.

Inman, D.L., Guza, R.T., 1982. The origin of swash cusps on beaches. Marine Geology 49, 133–148.

Jefferson, M.S.W., 1899. Beach cusps. Journal of Geology 7, 237–246.

Johnson, D.W., 1910. Beach cusps. Geological Society of America Bulletin 21, 599–624.

Johnson, D.W., 1919. Shore Processes and Shoreline Development. Wiley New York, 584 pp.

Komar, P.D., 1973. Observations of beach cusps at Mono Lake, California. Geological Society of America Bulletin 84 (11), 3593–3600.

Kuenen, P.H., 1948. The formation of beach cusps. Journal of Geology 56, 34–40.

Lippmann, T.C., Holman, R.A., 1989. Quantification of sand bar morphology: a video technique based on wave dissipation. Journal of Geophysical Research 94 (C1), 995–1011.

Longuet-Higgins, M.S., Parkin, D.W., 1962. Sea waves and beach cusps. The Geographical Journal 128 (2), 194–201.

Nishi, R., Sato, M., 1991. Photographic observation on cusps and wave fields. Conf on Coastal Engineering. Japan Society of Civil Engineers, Japan, pp. 296–300.

Palmer, H.R., 1834. Observations on the motions of shingle beaches. Philosophical Transactions of the Royal Society 124, 567–576.

Rasch, M., Nielsen, J., Nielsen, N., 1993. Variations of spacings between beach cusps discussed in relation to edge wave theory. Geografisk Tidsskrift 93, 49–55.

Resio, D.T., 1987. Extreme runup statistics on natural beaches. Miscellaneous Paper CERC-87–11, US Army Corps of Engineers, Waterways Experiment Station CERC, 29 pp.

Sato, M., Kuroki, K., Shinohara, T., 1992. A field experiment on the formation of beach cusps. In: Edge, B.L. (Ed.), ICCE 92, ASCE, Venice, Italy, pp. 2205–2218.

Shepard, F.P., 1938. Beach cusps and tides, a discussion. American Journal of Science Ser. 5, 35 (208), 309–310.

Shepard, F.P. 1963 Submarine Geology, 2nd ed. Harper and Row, New York, 557 pp.

Sloop, R.V., 1995. Beach cusp analysis and the dry beach evolution of Longboat Key, Florida using video monitoring techniques. M.E. Thesis, University of Florida, Gainesville, 104 pp.

Timmermans, P.D., 1935. Proeven over den invloed van golven op een strand. Leidsche Geologische Mededelingen 6, 380–386 (English Summary).

Werner, B.T., Fink, T.M., 1993. Beach cusps as self-organized patterns. Science 260 May 14 '93. 968–971.

Wright, L.D., Chappell, B.G., Thom, B.G., Bradshaw, M.P., Cowell, P. 1979. Morphodynamics of reflective and dissipative beach and inshore systems: southeastern Australia. Marine Geology 32, 105–140.